rms absorption. There is also doubt that Wannier levels can be observed in CdS, owing to the large exciton binding energies.[2] Finally, since a time average of data must be taken at these small $\Delta\alpha$ levels in order to eliminate noise, heating of the sample can cause serious error unless the field is turned off except during the actual measurement time.[4] Errors of this latter type increase the vertical error bar dramatically through the temperature dependence of E_g.

CONCLUSIONS

The results of these experiments clearly indicate the existence of very small field- and temperature-dependent oscillations. These oscillations agree well with the Callaway theory for Wannier levels if the light- and heavy-hole transitions are considered to be independent and if the results are averaged proportional to the effective masses (density of states) of each band.

In addition to the small Wannier oscillations, longer-period temperature-independent and sample-dependent (for amplitude) oscillations were also observed. It is believed that these oscillations are those observed by French[5] and Vavilov *et al.*[7]

---

†Work supported in part by the U. S. Air Force, under Grant No. AF-AFOSR-1157-66 and NASA institutional grants; done in partial fulfillment of the requirements for the Ph.D. by R. W. Koss at the University of Vermont.

*Permanent address: University of Vermont, Burlington, Vt.

[1]J. Callaway, Phys. Rev. 130, 549 (1963).

[2]For an analytical treatment see, e.g., C. B. Duke and M. E. Alferieff, Phys. Rev. 145, 583 (1966); H. I. Ralph, J. Phys. C 1, 378 (1968). For the case where excitons cannot be ignored (i.e., in CdS) see L. M. Lambert, Bull. Am. Phys. Soc. 14, 248 (1969).

[3]For a discussion of this specifically for *p*-type Ge see W. E. Pinson and R. Bray, Phys. Rev. 136, A1449 (1964).

[4]L. M. Lambert, J. Phys. Chem. Solids 26, 1409 (1965); Phys. Rev. 138, A1569 (1965).

[5]B. T. French, Phys. Rev. 174, 991 (1968).

[6]E. G. S. Paige and H. D. Rees, Phys. Rev. Letters 16, 444 (1966).

[7]V. S. Vavilov, V. B. Stopachinskii, and V. Sh. Chanbarisov, Fiz. Tverd. Tela 8, 2660 (1966) [Sov. Phys. Solid State 8, 2126 (1967)].

[8]The effective masses for GaAs proposed by R. W. Shaw [Phys. Rev. B 3, 3283 (1971)] were used for these calculations.

PHYSICAL REVIEW B VOLUME 5, NUMBER 4 15 FEBRUARY 1972

Low-Temperature Scattering in InSb Measured by Infrared Faraday Rotation*

T. O. Poehler and C. H. Wang
Applied Physics Laboratory, The Johns Hopkins University, Silver Spring, Maryland 20910
(Received 16 September 1971)

Low-temperature electron-impurity scattering has been measured in *n*-type InSb using both far-infrared Faraday rotation and ellipticity. The experimental results at 5 °K using 337- and 119-μm radiation yielded scattering times of $3-5\times10^{-12}$ sec, which are in good agreement with earlier measurements of scattering using cyclotron resonance linewidths. The results show that dc theory cannot be used to describe this experimental regime, but must be replaced by a more complete frequency-dependent theory of Coulomb interactions.

INTRODUCTION

The low-temperature dc conductivity of compound semiconductors, such as InSb, is governed by phonon scattering down to about 60 °K, while below this temperature ionized impurity scattering dominates. One might expect these mechanisms to operate at infrared wavelengths, since measurements of scattering times in some materials at high microwave frequencies have yielded the same values as deduced from dc measurements.[1,2] However, recent measurements of low-temperature electron-impurity scattering times in compound semiconductors using millimeter and infrared cyclotron resonance linewidths have yielded scattering times greatly in excess of those determined by dc mobility measurements.[3-5] It would appear desirable to make independent determinations of these scattering times which are not necessarily related to a resonant process for comparison with the results of the linewidth measurements. The free-carrier Faraday effect provides an excellent method for measuring low-temperature scattering over a wide range of magnetic fields. The Faraday effect has been widely used to measure the effective mass of free carriers in many compound semiconductors.[6] Use

of the measurement as a means of determining scattering times has been less frequent, and has not been generally carried out under the experimental conditions where the anomalies have been observed by cyclotron resonance.

This paper reports on the measurement of Faraday rotation and ellipticity in InSb using several infrared laser wavelengths. The results of these experiments have been analyzed by fitting the experimental data to calculated curves over a wide range of magnetic field including the region of cyclotron resonance. The work yields electron-impurity scattering times in close agreement with those measured from cyclotron resonance linewidths on the same samples.

THEORY

An electromagnetic wave propagating through a semiconductor at low temperatures can be considered to be traversing a plasma consisting of the free carriers with a background of positive ions. Wave propagation in this ionized magnetized dispersive medium is described by the plasma dielectric tensor and the dispersion equations. If the wave propagating through the system represented by

$$\vec{E}(\vec{r}, t) = \vec{E}(\vec{q}, \omega)\, e^{i(\vec{q}\cdot\vec{r}-\omega t)} \tag{1}$$

is traveling along the direction of an homogeneous magnetic field and the material has at least threefold symmetry about this axis, the dielectric tensor is given by

$$\epsilon = \begin{bmatrix} \epsilon_{xx} & -\epsilon_{xy} & 0 \\ \epsilon_{xy} & \epsilon_{xx} & 0 \\ 0 & 0 & \epsilon_{zz} \end{bmatrix} . \tag{2}$$

Here the z axis is chosen to be both the propagation direction of the electromagnetic wave and the direction of the magnetic field. The elements of interest in this Faraday geometry are

$$\epsilon_{\pm} = \epsilon_{xx} \pm i\epsilon_{xy} \tag{3}$$

with the plus and minus signs corresponding to right and left circularly polarized waves, respectively. In this convention, an electric vector with right polarization rotates in the same direction as do electrons in a magnetic field. In terms of the complex index of refraction $(n + i\kappa)$, the dispersion relations for the Faraday geometry ($\vec{q} \parallel \vec{B}$) are

$$(n_{\pm} + i\kappa_{\pm})^2 = \epsilon_{\pm} . \tag{4}$$

The rotation of the plane of polarization of a linearly polarized beam arises from the different phase velocities of the two circular components as they propagate through the medium. Over a path length l through the medium, the plane of polarization has undergone a rotation θ given by

$$\theta = (\omega l / 2c)(n_- - n_+) , \tag{5}$$

where ω is the angular frequency of the radiation. In addition to this effect, there is a corresponding differential absorption effect depending on $\kappa_{\pm}$. One of the circular modes can be attenuated more than the other causing the transmitted beam to be elliptically polarized. The ellipticity, which is defined as the ratio of minor to major axis of the ellipse of polarization, is given by

$$\Delta = \tanh\left(\frac{\omega l}{2c}(\kappa_- - \kappa_+)\right) . \tag{6}$$

The quantum formulation for the plasma dielectric tensor developed earlier for interpreting far-infrared cyclotron resonance measurements can be used to describe this case.[5] The dielectric tensor elements are

$$\epsilon_{\pm} = \epsilon_l\left[1 - \frac{\omega_p^2}{\omega^2}\left(1 + \frac{m^*\omega_c}{4\pi^2\hbar N}\sum_{\substack{n=0 \\ s=\mp}}(n + \tfrac{1}{2} \pm \tfrac{1}{2}) \times \int_{-\infty}^{\infty} \frac{\Delta f_0\, dk_z\, \omega_{n+1,n}}{\omega_{n\pm1,n} - \omega + i/\tau}\right)\right] , \tag{7}$$

where n is the initial Landau quantum number, s is the spin index, ϵ_l is the lattice dielectric constant, and τ is the electron-ion collision time. Here the plasma frequency ω_p is given by $\omega_p^2 = 4\pi Ne^2/\epsilon_l m^*$, where N is the electron density, e is the electronic charge, and m^* is the effective electron mass. The cyclotron frequency $\omega_c = eB/m^*c$, where B is the magnetic field. The resonant denominator of the integral in Eq. (7) contains the resonant frequency $\omega_{n+1,n}$ which can be expressed in terms of the conduction-band energy levels as

$$\omega_{n+1,n} = (1/\hbar)\,[\mathcal{E}(n+1, k_z, s) - \mathcal{E}(n, k_z, s)] . \tag{8}$$

In terms of the band gap $\mathcal{E}_g$ and the electron wave-vector component along the magnetic field direction k_z, the energy levels are given by

$$\mathcal{E}(n, k_z, s) = \tfrac{1}{2}\mathcal{E}_g\left\{-1 + \left[1 + \frac{4}{\mathcal{E}_g}\left(\frac{\hbar^2 k_z^2}{2m^*} + \hbar\omega_c\,(n + \tfrac{1}{2} + \tfrac{1}{2}\nu)\right)\right]^{1/2}\right\} , \tag{9}$$

where the parameter $\nu = gm^*/2m$ relates to the g factor. The electron distribution is considered to be described by the Fermi function $f_0(n, k_z, s)$ with Δf_0 defined as

$$\Delta f_0 = f_0(n', k_z + q_z, s) - f_0(n, k_z, s) . \tag{10}$$

The form of plasma dielectric tensor given by Eq. (7) has been used to compute the theoretical curves described in this work.

A less-exact description for the charge carriers

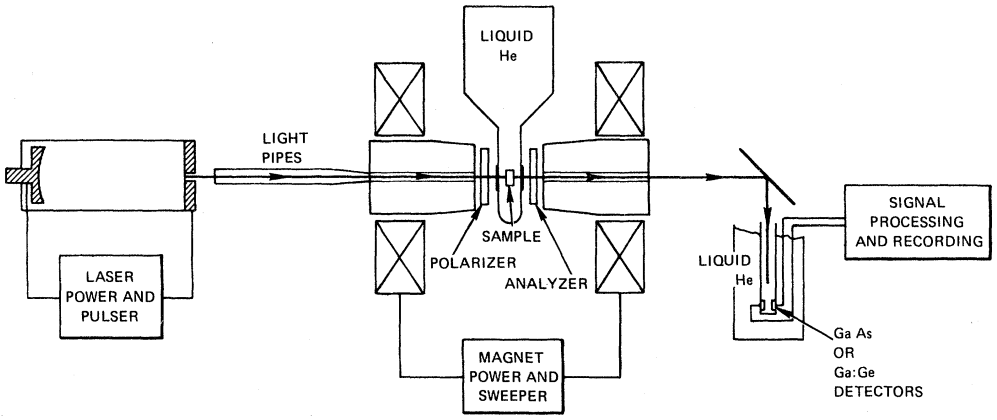

FIG. 1. Schematic of experimental apparatus for measuring Faraday rotation and ellipticity.

is given by the cold classical plasma dielectric tensor

$$\epsilon_{\pm} = (n_{\pm} + i\kappa_{\pm})^2 = \epsilon_l \left\{ 1 - \frac{\omega_p^2}{\omega(\omega + \omega_c - i/\tau)} \right\} . \qquad (11)$$

If the conditions $\omega \gg \omega_p$ and $|\omega - \omega_c|\tau \gg 1$ are satisfied, the angle of rotation of the plane of polarization is given by the approximation

$$\theta = \frac{\epsilon_l^{1/2} \omega_p^2 \omega_c l}{2c(\omega^2 - \omega_c^2)} . \qquad (12)$$

Under these conditions the ellipticity Δ can be expressed as

$$\Delta = \frac{\epsilon_l^{1/2} \omega_p^2 \omega \omega_c l}{c(\omega^2 - \omega_c^2)^2 \tau} , \qquad (13)$$

where it is also assumed that $\omega l (\kappa_- - \kappa_+) 2c \ll 1$. The ratio θ/Δ is given by

$$\theta/\Delta = \tfrac{1}{2}\omega\tau [1 - (\omega_c/\omega)^2] \qquad (14)$$

for values of ω away from resonance. The ratio θ/Δ can be used as a measure of the electron-ion scattering time τ. In many cases, particularly near cyclotron resonance, exact expressions for the rotation and ellipticity must be computed to obtain reasonable agreement with experimental results.

EXPERIMENT

The measurements of Faraday rotation and ellipticity were conducted using the arrangement shown schematically in Fig. 1. Far-infrared radiation was generated using a gas laser system which has been described in previous publications.[7-9] The laser was a 2.3-m-long 15-cm-diam device of semiconfocal optical configuration which was pulsed at 23 pulses/sec with a 5-kV capacitor discharge. The far-infrared radiation used in the experiments reported here was the 118.6-μm water-vapor emission line and the 336.8-μm HCN line. The laser radiation was extracted from the cavity through a 6-mm coupling hole covered by a 3-mil-thick polyethylene window. The beam was transmitted through light pipes of 1.25-cm diam to a 6.25-mm-diam hole bored along the axis of the magnet-pole piece. The beam was then polarized by an infrared grating polarizer before being transmitted through the sample. Upon emerging from the sample, the beam passed through a rotatable grating polarizer used as an analyzer. The transmitted signal was measured by means of either a GaAs- or Ga-doped Ge photoconductive cooled detector.

The far-infrared polarizers were vacuum-evaporated aluminum transmission gratings with lines spaced approximately 25 μ apart on either Mylar or silicon substrates. The degree of polarization of these elements was approximately 93% at both wavelengths of interest.

The rotation and ellipticity data were obtained from high-purity n-type InSb samples, of volume $8\times9\times1$ mm^3, cut normal to the [111] axis and etched in the acid etch CP-4 to the desired thickness. The 77 °K electron concentration of this material was 1×10^{14} cm^{-3} with dc mobility $\mu_0 = 6.7 \times 10^5$ cm^2/V sec. The sample was mounted in an aperture in a copper block and cooled by conduction to 5 °K as measured by a semiconductor sensor. The optical windows in the Dewar tail were the visible and far-infrared transmitting material TPX.[10]

The 337-μm radiation was detected with a 100-μm-thick n-type GaAs epitaxial detector with room-temperature carrier concentration of 2×10^{15} cm^{-3} and mobility of 7000 cm^2/V sec; sample resistance at 4.2 °K was 1.4×10^5 Ω. Ohmic contacts were made to the detector by alloying Au-Sn vacuum-deposited contacts at 400 °C. The photoconductive signal was observed by the change in voltage across the 2×8-mm^2 rectangular sample when biased with 40 μA from a constant-current source.

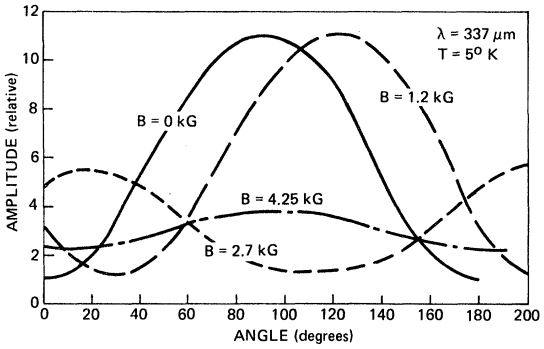

FIG. 2. Infrared transmission of InSb specimen as a function of angle between polarizer and analyzer for several values of magnetic field. The progressive rotation and increase in ellipticity of the beam is clearly illustrated.

Larger bias values produce noise, and ultimately impact ionization at field strengths of approximately 7.5 V/cm. The 119-μm line emitted by water vapor was detected using a Ga-doped Ge photoconductor. This detector had an impurity concentration of 1×10^{14} cm^{-3} so that at 4.2 °K the $2\times2\times8$-mm^3 sample had a resistance of 200 kΩ. The maximum bias on this element was restricted to about 20 μA by the critical field for impact ionization at 5 V/cm. The output signals from these detectors were processed by a preamplifier, a gated integrator, and synchronous phase-coherent detector, and were recorded as a function of analyzer rotation angle. The limiting noise in the system came from amplitude fluctuations in the laser output which were several percent of the peak signal.

EXPERIMENTAL RESULTS

The far-infrared beam transmitted through the polarizer, analyzer, and experimental sample varies periodically as a function of the rotation angle of the analyzer with a period of π rad as illustrated in Fig. 2. If two imperfect polarizers are used to produce the transmission curve, the minima do not reach zero. The percentage polarization P of either polarizer may be measured in terms of the intensity ratio I_{max}/I_{min} which for $I_{max} \gg I_{min}$ is given by[6]

$$P = \frac{2I_{max} - I_{min}}{2I_{max} + I_{min}} . \tag{15}$$

When the magnetic field is applied to the specimen, the plane of polarization of the beam is rotated producing the curves also shown in this figure. The shift in the point of maximum or minimum intensity is taken as the rotation angle θ. When the plane-polarized radiation becomes elliptical as a result of scattering, the ratio between maxima and minima becomes smaller. The ellipticity Δ is then given by the expression

$$\Delta^2 = (M - X)/(MX - 1) , \tag{16}$$

where M is the intensity ratio of minimum to maximum in zero field and X is the same ratio in the magnetic field.

Analysis of the data as shown in Fig. 2 leads to measurements of the rotation and ellipticity at $\lambda = 337$ μm as a function of magnetic field as shown in Figs. 3 and 4. The rotation increases with field up to the resonant field strength where there is a sign reversal, followed by a decrease in rotation angle. The experimentally observed ellipticity reaches a maximum near the resonant magnetic field, but the maximum and minimum intensity values do not become equal at resonance as predicted by the computation. Also shown in Figs. 3 and 4 are curves calculated using the exact expression for the quantum plasma dielectric tensor with different values of relaxation times τ. Calculations

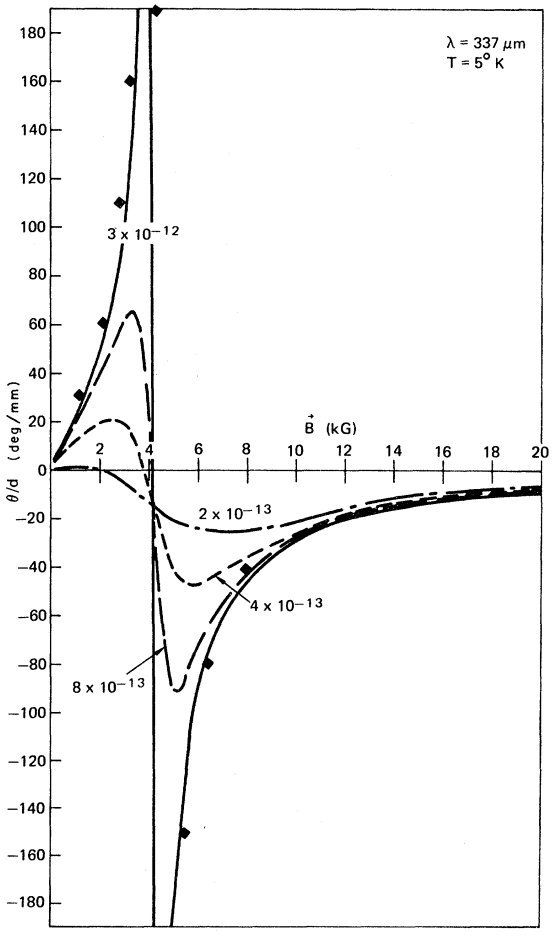

FIG. 3. Measured Faraday-rotation angle as a function of magnetic field at 337 μm. Curves are calculated from Eqs. (5)–(7) for different values of scattering time. Experimental data shown as solid squares.

made using the cold-plasma tensor elements were in fairly good agreement with the exact formulation at 5 °K although the ellipticity above resonance differed considerably. These differences are accentuated at higher temperatures where the cold plasma tensor becomes increasingly less representative. It appears that a good fit to the experimental rotation data is obtained for a relaxation time of approximately 3×10^{-12} sec. There is a serious difference in the measured and computed ellipticity values near the cyclotron resonance field. A similar discrepancy has been observed by other experimenters in higher-temperature measurements.[11] Analogous results are obtained in warm gas plasmas as a result of the partial cancellation of the collisional effects by effect of temperature on the propagation of the right-handed wave near cyclotron resonance.[12] In the regions away from the resonant field, however, the ellipticity data also appear to match reasonably well with the curve for $\tau = 3\times10^{-12}$ sec.

A similar series of measurements were made using the 119-μm water-vapor emission line. The rotation and ellipticity determined from these measurements are shown in Figs. 5 and 6 together with calculated curves for various values of relaxation time. The rotation data seems to fit well with a τ of 5×10^{-12} sec, while the ellipticity results best match a relaxation time of 3×10^{-12} sec. In this experiment, the whole range of the rotation curve could not be measured due to a maximum available field of 11.5 kG for this electromagnet.

DISCUSSION

The electron-ion impurity-scattering times measured by the far-infrared Faraday-rotation experiments yield values in the range $3-5\times10^{-12}$ sec. These measurements are in sharp contrast to the field-dependent dc scattering time $\tau_0(B)$. This parameter varies from $\tau_0(B=0) = 7\times10^{-13}$ sec to $\tau_0(B = 10\text{ kG}) = 6\times10^{-14}$ sec with an asymptotic behavior approximately given by $1/B$. There is good agreement between the scattering times from the rotation measurements and those derived from cyclotron resonance linewidths using the same radiation frequencies.[4,5] The cyclotron resonance measurements yielded scattering times at wavelengths of 337 and 119 μm, respectively, of 2.8×10^{-12} and 5.3×10^{-12} sec.

Electron-ion collisions in InSb at low temperature in a strong magnetic field and in the quantum limit ($\hbar\omega_c \gg k_B T$) as measured in these experiments are qualitatively different from the classical dc impurity scattering. The electron-ion interaction must be described in terms of frequency-dependent Coulomb scattering. For low magnetic fields where the cyclotron orbit radius ($r_c = \hbar c/eB$) is greater than the shielding length $1/k_s$ there is a short-range in-

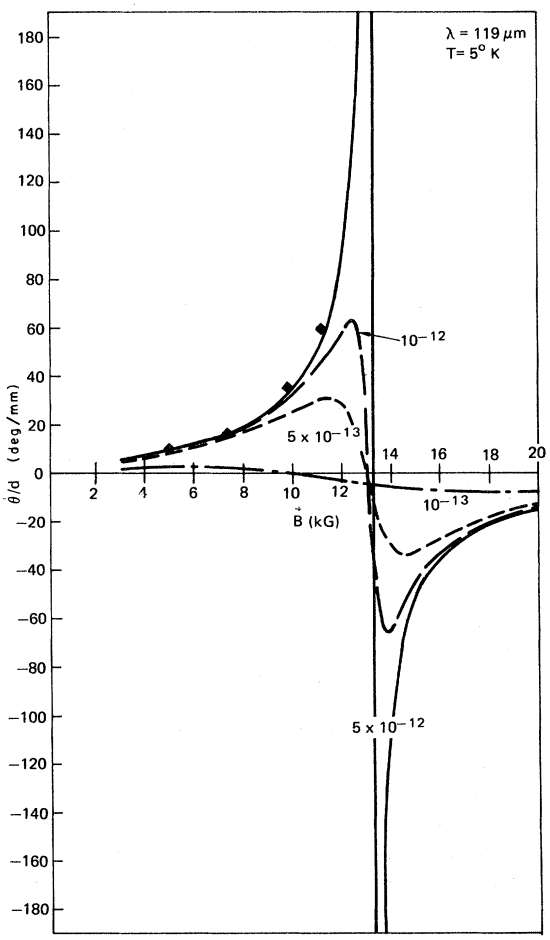

FIG. 5. Faraday rotation measured in InSb at 119 μm.

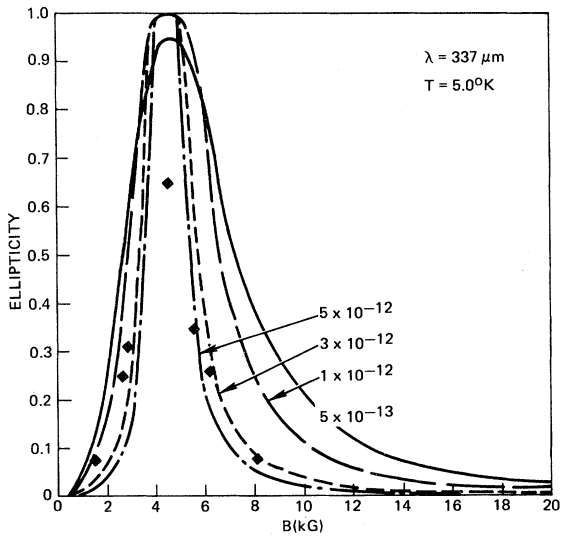

FIG. 4. Observed ellipticity as a function of magnetic field at 337 μm compared with calculated curves.

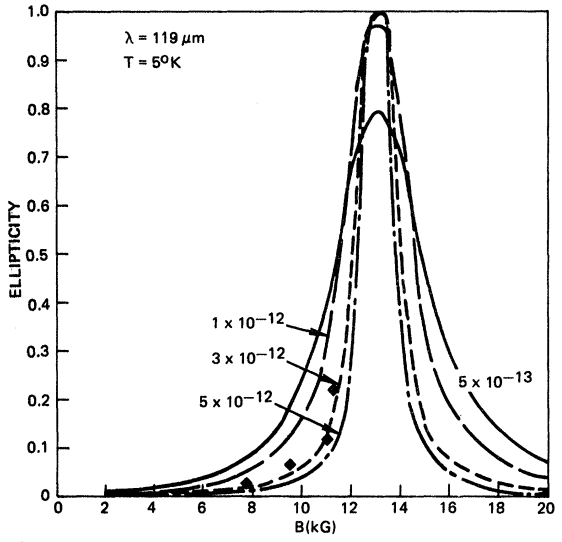

FIG. 6. Observed ellipticity vs magnetic field at 119 μm.

teraction. The interaction is governed by a shielded ionized impurity potential behaving as

$$U(r) = e^2 e^{-k_s r}/\epsilon_l r \ , \tag{17}$$

where the shielding distance is either the Debye length $1/k_s = \epsilon_l k_B T/4\pi m_c e^2$, or the Fermi-Thomas length $1/k_s = \epsilon_l \zeta_0/6\pi n_c e^2$ depending on whether the electron statistics are classical or degenerate.

The case of a long-range impurity interaction for which $r_c \ll 1/k_s$ is qualitatively different. The scattering may be nonadiabatic where an electron-ion collision causes an electron to redistribute its total energy among its internal states with little energy exchange to the heavy particle. Kawabata has calculated a transport relaxation time $\tau_{\text{nonad}}(\omega_c)$, which for photon frequencies near ω_c is[13]

$$\tau_{\text{nonad}}(\omega_c) = \epsilon_l^{\,2} \hbar\omega_c \left| \hbar k_z \right| 2\pi N_i e^4 \ . \tag{18}$$

This scattering involves only the z component of momentum and grows with increasing B.

At higher values of B, the scattering is dominated by an adiabatic rate $1/\tau_{\text{ad}}(\omega_c)$ resulting from electron drift motion in the combined external magnetostatic field and the impurity electrostatic field E_i. The drift motion modulates the electron cyclotron frequency, introducing a frequency spread into the spectrum. Using the appropriate averages, the reciprocal of the frequency spread becomes $\tau_{\text{ad}}(B)$ given by[14,15]

$$\tau_{\text{ad}}(\omega_c) = \left(\frac{15}{4\pi N_i}\right)^{1/2} \frac{\epsilon_l}{e^2 (m\hbar^2\omega_c)^{1/4}} \ , \tag{19}$$

a very weak dependence on frequency or magnetic field. Recent calculations of infrared cyclotron resonance linewidths at low temperatures in nondegenerate systems using different forms of long-range electron impurity interactions using the Kubo theory have yielded results similar to Kawamura for the case of unshielded Coulomb potentials.[16] However, using various forms of shielded interaction, the high-frequency resonance linewidths reach constant values in the long-range limit. Both of the processes described by Eqs. (18) and (19) occur simultaneously with the dominance of one or the other being determined by experimental conditions, and so the total scattering time is given by the harmonic sum

$$1/\tau(\omega_c) = 1/\tau_{\text{nonad}}(\omega_c) + 1/\tau_{\text{ad}}(\omega_c) \ . \tag{20}$$

The appropriateness of the expression given by Eq. (20) in describing scattering as measured by far-infrared radiation may be judged by results shown in Table I. In this table the high-frequency scattering times measured by cyclotron resonance experiments[5] $\tau_{\text{CR}}(\omega_c)$, and by infrared Faraday rotation $\tau_{\text{FR}}(\omega_c)$ and ellipticity $\tau_{\text{EL}}(\omega_c)$, are compared with the scattering time computed from the frequency-dependent Coulomb scattering time $\tau_{\text{COMP}}(\omega_c)$. The agreement between these parameters contrasts sharply with the field-dependent dc scattering time $\tau_0(B)$. The Faraday-rotation results for each wavelength used in the experiment appeared to be well fitted by a single scattering time although the magnetic field varied over a wide range; the ellipticity at 337 μm was somewhat less regular at low magnetic fields. The former would seem to imply that the scattering times should be considered to be frequency-dependent parameters. The expressions for adiabatic and nonadiabatic Coulomb scattering in the quantum limit [Eqs. (18)–(20)] appear to correctly represent ionized impurity scattering for energies above the plasmon energy.

TABLE I. Scattering times in InSb.

$\lambda_c(\mu\text{m})$	336.8	118.6
$\tau_{\text{CR}}(\omega_c)$ (sec)	2.8×10^{-12}	5.3×10^{-12}
$\tau_{\text{FR}}(\omega_c)$ (sec)	3×10^{-12}	5×10^{-12}
$\tau_{\text{EL}}(\omega_c)$ (sec)	3×10^{-12}	3×10^{-12}
$\tau_{\text{COMP}}(\omega_c)$ (sec)	3.1×10^{-12}	5.5×10^{-12}
$\tau_0(B)$ (sec)	2×10^{-13}	7×10^{-14}

*Work supported by the Department of the Navy under Contract No. N00017-62-c-0604.

[1]D. M. S. Bagguley, R. A. Stradling, and J. S. S. Whiting, Proc. Roy. Soc. (London) 262, 340 (1961).
[2]D. M. S. Bagguley, M. L. A. Robinson, and R. A. Stradling, Phys. Letters 6, 143 (1963).
[3]J. M. Chamberlain and R. A. Stradling, Solid State Commun. 7, 1275 (1969).
[4]J. R. Apel, Jr., T. O. Poehler, and C. R. Westgate, Solid State Commun. 8, 1693 (1970).
[5]J. R. Apel, Jr., T. O. Poehler, C. R. Westgate, and R. I. Joseph, Phys. Rev. B 4, 436 (1971).
[6]E. D. Palik, Appl. Opt. 2, 527 (1963).
[7]R. Turner, A. K. Hochberg, and T. O. Poehler, Appl. Phys. Letters 12, 104 (1968).
[8]R. Turner and T. O. Poehler, J. Appl. Phys. 39, 5726 (1968).
[9]J. R. Apel, T. O. Poehler, and C. R. Westgate, Appl. Phys. Letters 14, 161 (1969).
[10]G. W. Chantry, H. M. Evans, J. W. Fleming, and H. A. Gebbie, Infrared Phys. 9, 31 (1969).
[11]M. Shimura, N. Takeuchi, and T. Yajima, Japan. J. Appl. Phys. 9, 1334 (1970).
[12]M. A. Heald and C. B. Wharton, *Plasma Diagnostics with Microwaves* (Wiley, New York, 1965), p. 108.
[13]A. Kawabata, J. Phys. Soc. Japan 23, 999 (1967).
[14]H. Kawamura, H. Saji, M. Fukai, K. Sekido, and I. Imai, J. Phys. Soc. Japan 19, 288 (1964).
[15]S. J. Miyake, J. Phys. Soc. Japan 20, 412 (1965).
[16]E. E. H. Shin (private communication).

PHYSICAL REVIEW B VOLUME 5, NUMBER 4 15 FEBRUARY 1972

Matrix Elements in Interband Optical Transitions*

J. P. Van Dyke
Sandia Laboratories, Albuquerque, New Mexico 87115
(Received 18 October 1971)

We have calculated the imaginary part of the dielectric constant ϵ_2 for Si and Ge using interband matrix elements obtained from the full orthogonalized-plane-wave (OPW) wave function (rather than only the plane-wave portion). The results show that for the class of semiconductor represented by Si and Ge a pseudopotential description including pseudo-wave-function matrix elements is quite adequate for obtaining the one-electron transition probabilities.

INTRODUCTION

Over the last nine years, theoretical calculations of the imaginary part of the dielectric constant ϵ_2 have been carried out for a large number of semiconductors. The calculations have employed a variety of methods including pseudopotential,[1-3] full zone $\vec{k}\cdot\vec{p}$,[4,5] and Fourier expansion (tight binding).[6] From the outset the importance of the interband matrix elements has been recognized.[7] For each method there is a prescription for obtaining the matrix elements.[8] For the above methods the prescriptions are equivalent to defining the interband velocity operator[9] as the k-space gradient acting on the model Hamiltonian,

$$\vec{v}(\vec{k}) = \vec{\nabla}_{\vec{k}}\mathcal{H}(\vec{k}) . \tag{1}$$

With the exception of one PbTe calculation,[5] matrix elements calculated from first principles have never been employed. (Unfortunately, in that case the calculated ϵ_2 differs from the experimental ϵ_2 by a factor of 2.[10]) In the most commonly used technique, the local-pseudopotential method, there are terms in the full wave function which are omitted in the pseudopotential-matrix-element calculation. These terms have been calculated at Γ in the Brillouin zone in a few materials[11,12] and found to generally contribute 20% or less to the matrix element. We present here the results of ϵ_2 calculations in which the full OPW wave function has been used to calculate the interband matrix elements for the well-understood semiconductors Si and Ge. We will show that the difference from pseudopotential matrix elements is really quite small. Finally, to emphasize the distinction between Eq. (1) and the (real-space) gradient acting on a pseudo-wave-function, we will discuss matrix elements in copper derived from a nonlocal pseudopotential employing three different prescriptions.

METHOD

The present work starts with an OPW calculation including velocity matrix elements. The crystal potential used is a superposition of spherically symmetric self-consistent free-atom potentials.[13] The Kohn-Sham-Gaspar value $\frac{2}{3}$ is used for the coefficient of the Hartree-Fock-Slater free-electron exchange. Approximately 181 OPW's are employed throughout. This simple model gives eigenvalues within a few tenths of an eV of the experimental values. The OPW calculation was carried out at points Γ, X, L, and W in the Brillouin zone for Ge and Si plus $\Delta(\frac{1}{2}00)$ and $\Sigma(\frac{1}{2}\frac{1}{2}0)$ in Si. The OPW eigenvalues and velocity matrix elements were then used in a parameterless $\vec{k}\cdot\vec{p}$ extrapolation to provide energies and matrix elements throughout the